The effect of a roundabout corridor's design on selecting the optimal crosswalk location: a multi-objective impact analysis

Fernandes P. a*, Salamati, K b, Coelho, M.C. a, Rouphail, N.M b

a Department Mechanical Engineering / Centre for Mechanical Technology and Automation (TEMA), University of Aveiro, Campus Universitário de Santiago, 3810-193 Aveiro - Portugal

b Institute for Transportation Research and Education/ North Carolina State University, North Carolina State University, Campus Box 8601, Raleigh, NC 27695-8601

* PhD Student, Mechanical Engineering, E-mail: paulo.fernandes@ua.pt

University of Aveiro, Dept. Mechanical Engineering / Centre for Mechanical Technology and Automation (TEMA), University of Aveiro, Campus Universitário de Santiago, 3810-193 Aveiro - Portugal

ABSTRACT

Crosswalks located at mid-block segment between roundabouts can provide a good balance among delay, carbon dioxide (CO_2) emissions and relative difference between vehicles and pedestrians speed. However, when considering local pollutant criteria, the optimal crosswalk location may be different to that obtained for CO_2.

This paper described a multi-objective analysis of pedestrian crosswalk locations, with the objectives of minimizing delay, emissions and relative difference between vehicles and pedestrians speed. Accounting for the difference between global (e.g. CO_2) and local pollutants (monoxide carbon, nitrogen oxides and hydrocarbons) was one the main considerations of this work. Vehicle activity along with traffic and pedestrian flows data at six roundabout corridors in Portugal, one in Spain and one in the US were collected and extracted. A simulation environment using VISSIM, VSP, and SSAM models was used to evaluate traffic operations along the sites. The Fast Non-Dominated Sorting Genetic Algorithm (NSGA-II) was implemented to further search optimal crosswalk locations.

The results yielded improvements to both delay and emissions by using site-optimized crosswalks. The findings also revealed that the spacing between intersections widely influenced the optimal crosswalk location along a mid-block section. If the spacing is low (<100 m), the crosswalk location will be approximately in 20%-30% of the spacing length. For spacing values between 140 and 200 m, crosswalks would be located at the midway position. When a specific pollutant criterion was considered, no significant differences were observed among optimal crosswalk data sets.

Keywords: CO_2, Crosswalks, Local pollutants, Multi-objective optimization, Roundabout Corridors, Spacing

Introduction and Literature Review

In the past few decades, many transportation authorities are progressively looking at roundabouts as an alternative solution to signalized intersections as a means to improve traffic performance, and safety for vulnerable road users such as pedestrians **(Brilon, 2016; NCHRP, 2010).** This trend has prompted the increased construction of roundabout corridors across Europe and in the United States (US). Many of these corridors are placed in commercial and residential neighborhoods, where some pedestrian activity is expected.

Previous studies have documented the influence of pedestrian streams on available vehicular capacity of the isolated roundabouts **(Hellinga & Sindi, 2012; Kang & Nakamura, 2015; Kang, Nakamura, & Asano, 2014; Schroeder, Rouphail, Salamati, & Bugg, 2012; Żak, Meneguzzer, & Rossia, 2011)**. Some authors suggest locating the crosswalks 10 to 15 m downstream of the exit junction in order to improve traffic operations **(HCM, 2010; Silva, Cunha, Relvão, & Silva, 2013)**. Duran and Cheu (2013) stated that entry capacity was negatively influenced by short distances between the crosswalk and the yield line. However, the afro-mentioned studies only included the analysis of crosswalks at roundabouts in isolation.

Roundabout corridors have specific operational characteristics compared with roundabouts in isolation. Fundamentally, high congested mid-block areas between adjacent roundabouts in close-proximity substantially impact vehicle speed and acceleration-deceleration patterns **(Isebrands, Hallmark, Fitzsimmons, & Stroda, 2008)**, as well as pollutant emissions on the adjacent roundabouts **(Fernandes, Salamati, Rouphail, & Coelho, 2015)**. Thus, the impact of the pedestrian crosswalks on corridors capacity may arise under conditions of short spacing intersections.

The research on traffic performance, fuel consumption and emissions in corridors with different traffic controls is extensive but did not include the influence of pedestrian crosswalks **(Fernandes, Fontes, Neves, et al., 2015; Guo & Zhang, 2014; Haley et al., 2011; Silva, Mariano, & Silva, 2015)** or the impact of spacing on traffic operations **(Dhamaniya & Chandra, 2014; Kwak, Park, & Lee, 2012; Yang, Liu, Xu, & Xu, 2016).** Bugg et al. **(2015)** developed empirical models to predict arterial travel time and delay along roundabout corridors. These models neither assessed the impact of crosswalks on traffic operations nor included the emissions and safety fields on their equations.

The implementation of the crosswalk along the mid-block section between roundabouts could result in a trade-off among vehicle delay, safety and emissions. On the one side, a crosswalk near the roundabout has a negative impact on emissions and delays, and simultaneously can be safe for pedestrians since vehicles drive at low speeds. On the other side, crosswalks close to mid-block improve capacity and emissions, but could increase injury risk for pedestrians.

With these concerns in mind, **Fernandes, Fontes, Pereira, et al. (2015)** examined the integrated effect of crosswalk location between closely-spaced two-lane roundabouts (spacing <170 m) in the city of Chaves (Portugal) on traffic delay, carbon dioxide (CO_2) emissions and relative difference between vehicles and pedestrians speed. They found that locating the crosswalk at 15 and 55 to 60 m from the exit section provided a good balance among those outputs. The authors also recommended that the spacing between roundabouts constrained vehicle speeds at mid-block segments **(Fernandes, Fontes, Pereira, et al., 2015)**. Nevertheless, this study has two main limitations. First, one specific site was evaluated, which restricted the applicability of study's findings to other locations. Second, the authors did not assess the impacts of the crosswalk location on local pollutant emissions, which have direct effects on human health.

The available literature around this topic has focused on capacity/delay, emissions (only for CO_2 that is relevant for global warming) and safety fields separately or used limited study cases. Understanding the differences on optimal crosswalk locations between CO_2 and local pollutants in an integrated way is lacking. Still, none of the previous studies has addressed how optimal crosswalk location at mid-block segment is determined by corridor's design.

This paper discusses the integrated effect of pedestrian crosswalk location on vehicle delay, pedestrian safety, and emissions for pollutant criteria (CO_2, monoxide carbon – CO, nitrogen oxides – NO_X, and hydrocarbons – HC) in roundabout corridors. The research methodology is based on the work by **Fernandes, Fontes, Pereira, et al. (2015)**. The optimal crosswalk locations along mid-block sections were hypothesized to vary due to differences in: *1*) geometric design of roundabouts; *2*) roundabout spacing; and *3*) pollutant type. Thus, this research tested and verified these expectations in eight roundabout corridors from three different countries (Portugal, Spain and United States – US). Capacity, emissions and safety were used to explore the impact of crosswalk locations using a microscopic traffic model (VISSIM) together with a microscale emission methodology (Vehicle Specific Power – VSP) and safety model (Surrogate Safety Assessment Model – SSAM). A multi-objective genetic algorithm was mobilized to search site-optimal crosswalk locations, and subsequent results compared with existing crosswalk locations.

The novelty of this study is the distinction between global and local pollutants in the final set of optimal crosswalk locations along the mid-block section, and the relationship between such locations and the corridor's design features. Therefore, this paper intends to focus on the following research questions:

- What is the optimal crosswalk location with minimum vehicle delay, emissions (both global and local pollutants) and maximum safety for pedestrians?
- How spacing between roundabouts impacts on optimal crosswalk location?

Second section describes the methodology used in this research. Analysis results are explained in third section, followed by the main conclusions and the limitations of this research in fourth section.

Methodology

The proposed methodology is built on a microsimulation framework to evaluate the pedestrian crosswalk on vehicle delay, pollutant emissions, and pedestrian safety. The methodology was divided in the following steps (**Figure 1**). First, traffic and pedestrian flows, and GPS data were collected in the selected study sites. Second, each site was coded using VISSIM microscopic traffic model and calibrated according the site-specific characteristics. Third, several operational scenarios on each studied location were defined; for each scenario, emissions and safety were analyzed using VSP methodology and SSAM model. Step four focused on the description of the multi-objective procedure.

Figure 1 Methodological framework.

Field data collection and study sites

Data were collected at the candidate sites during the evening peak (4:00 to 6:00 p.m.) on typical weekdays (Tuesday to Thursday) from April to June 2015, and under dry weather conditions:

- Traffic flows (Passenger Vehicles, Heavy Duty Vehicles and Transit Buses);
- Pedestrian flows at the candidate crosswalks on both directions of travelling (4:00-6:00 p.m.);
- High resolution vehicle activity data (speed, acceleration-deceleration and road slope on a second-by-second basis);
- Time-gap distributions data;
- Spacing between roundabouts;
- Posted speed limits.

Traffic and pedestrian flows, and time-gap distributions data (gap-acceptance and gap-rejection) for all turning maneuvers were collected from overhead videos installed at strategic points along the study sites. The recorded videotapes were later reviewed in research laboratory for obtaining traffic and pedestrian flows and resulting Origin-Destination (O-D) matrices. Data were recorded in 15-min time intervals. GPS Technology, in the form of an in-vehicle data logger, recorded the speed, position, latitude and longitude coordinates as well as topographic conditions of the vehicles as they traveled along the corridors (in 1-second time intervals). The GPS equipped-vehicle continuously loops through a pre-defined route extending beyond the beginning and end of the corridor (through movements).

To generalize the applicability of the methodology and range of the dataset, the authors selected sites for data collection representing a variety of characteristics and conditions. Using these considerations, six urban roundabout corridors in the North and Center of Portugal (PT1, PT2, PT3, PT4, PT5 and PT6), and one in Spain (SP1) and in the US (US1) were selected. The sites included the following range of attributes: *1*) number of roundabouts per corridor between 2 and 5; *2*) spacing ranged from 58 m to 200 m; and *3*) posted speed limits lower than 50 km/h.

The team elected one crosswalk at the corridors with 2 roundabouts (**Figure 2**a-e) and two crosswalks for other sites (**Figure 2**f-h). The pedestrian activity at other crosswalks did not affect site traffic operations (negligible pedestrian flows) and therefore was ignored. Almost sites are located on relatively flat grades. The exception was the PT4 site (**Figure 2**-f) where crosswalks were placed on a high slope arterial (>5%).

Table 1 lists each site where data were collected, including geographic location, number of approach lanes on the arterial, number of circulating lanes in the roundabouts, number of entry and exit legs, circle inscribed diameter, spacing between roundabouts (measured from the downstream exit lane from one roundabout to the upstream yield lane of the adjacent roundabout in the direction of travel) based on the procedures presented in the research of Bugg et al. (**2015**), presence of restrictive median, location for the candidate crosswalks from the circulatory ring delimitation, and crosswalk GPS coordinates.

The peak arterial traffic and pedestrian flows data are also presented in **Table 1**. 800 GPS travel runs for each through movement (around 100 at each site) were extracted and identified for this research (440 km of road coverage over 16 hours) (**S. Li, Zhu, van Gelder, Nagle, & Tuttle, 2002)**.

Figure 2 Aerial view of the Candidate Sites: a) US1; b) SP1; c) PT1; d) PT2; e) PT3; f) PT4; g) PT5; h) PT6 [Source: https://www.bing.com/maps/].

Table 1 Summary of Study Sites

Microsimulation platform for traffic, emissions, and safety

Traffic modelling

VISSIM software package was selected to simulate traffic operations **(PTV AG, 2011)** for four main reasons: *1*) modelling reliable pedestrian-vehicle interactions at roundabout corridors **(Fernandes, Fontes, Pereira, et al., 2015)**; *2*) defining parameters of driving behavior for roundabouts as critical gaps and headways **(Z. Li, DeAmico, Chitturi, Bill, & Noyce, 2013; PTV AG, 2011)**; *3*) calibrating a wide range of parameters to set faithful representations of the traffic on a corridor level for capacity and emissions' purposes **(Fernandes, Fontes, Neves, et al., 2015; Fernandes, Fontes, Pereira, et al., 2015)**; and *4*) storing and exporting of both vehicle and pedestrian trajectory files that can be used by external applications to assess emissions and safety **(PTV AG, 2011)**.

The simulation experiments in each site were based on simulation runs of 75 minutes (4:45-6:00 p.m.). A fifteen minutes (4:45-5:00 p.m.) warm-up time was included in each run to allow traffic to stabilize before collecting data for the remaining 60 minutes. The coded network in VISSIM is depicted in **Figure 2**. Link speeds and flows (traffic and pedestrian) were collected for all of these links. An average pedestrian walking speed value of 1.34 m/s was adopted for this research **(HCM, 2010)**.

Emissions

Vehicular emissions were calculated using VSP methodology **(USEPA, 2002)**. VSP, an indicator of engine load, accounts for engine power demand associated with changes in both vehicle potential and kinetic energies, aerodynamic drag, and rolling resistance **(Frey, Zhang, & Rouphail, 2010; USEPA, 2002)**. VSP values estimated at 1 Hz are categorized in 14 modes, and an emission factor for each mode is used to estimate vehicular CO_2, CO, NO_X and HC emissions from different vehicle types.

The main advantages of using VSP are: *1*) it allows estimating instantaneous emissions based on a second-by-second vehicle activity data, taking as input the trajectory files given by VISSIM; *2*) it includes the impact of different levels of accelerations and speed changes on emissions **(Kutz, 2008)**; *3*) and it is an useful explanatory variable for estimating variability in emissions **(Zhai, Frey, & Rouphail, 2008)**.

Thus, emissions estimates using VSP methodology were based on vehicle dynamic data (speed, acceleration-deceleration and slope) gathered from VISSIM. Excel data sheets were developed to compute second-by-second vehicle dynamics data from VISSIM output. To reflect the local car fleet compositions, the total emissions were calculated considering the following distributions:

- Portuguese Sites: 44% of Gasoline Passenger Vehicles (GPV) with engine size <1.4l, 35% of Diesel Passenger Vehicles (DPV) with engine size <1.6l, and 21% of Light Diesel Duty Trucks (LDDT) with engine size <2.5l **(ACAP, 2014)**;

- Spanish Site: 41% of Gasoline Passenger Vehicle (GPV) with engine size <1.2l, 51% of Diesel Passenger Vehicle (DPV) with engine size <1.6l, and 8% of and Light Diesel Duty Trucks (LDDT) with engine size <2.5l **(DGT)**;
- US Site: 39% of "Tier 1" Passenger Cars (T1 PCs) and 61% of "Tier 2" Passenger Cars (T2 PCs) **(OAK Bridge Data Inventory)**.

The average emission rates for pollutants CO_2, CO, NOx and HC by VSP mode of the above vehicles types are reported in the following studies: GPV **(Anya, Rouphail, Frey, & Liu, 2013)**, DPV and LDDT **(Coelho, Frey, Rouphail, Zhai, & Pelkmans, 2009)**, and T1 and T2 (PCs) **(Salamati, Rouphail, Frey, Liu, & Schroeder, 2015)**. Other categories represented only 2% of traffic composition and were excluded from this analysis.

Safety

SSAM software application was developed by a research team in SIEMENS and sponsored by the Federal Highway Administration (FHWA). SSAM uses several algorithms to identify conflicts from space-time vehicles trajectory files (*.trj file) produced by microscopic simulation modes as VISSIM. For each vehicle-to-vehicle (or pedestrian) interaction SSAM computes surrogate measures of safety and determines whether or not that interaction fulfils the criteria to be deemed a conflict **(Gettman, Pu, Sayed, & Shelby, 2008).**

This approach has all the common advantages of simulation such as safety evaluation of new facilities before their implementation, or controlled testing environments. However, notwithstanding the simplicity of user interface, SSAM has two main drawbacks. First, current microscopic traffic models are not able to model specific crash types such as head-on, sideswipe or U-turn related collisions. Second, the probability of each automated conflict turning into a crash cannot be determined by SSAM **(Gettman et al., 2008)**.

The research team used Time-to-Collision (TTC) as a threshold to establish whether a vehicle-pedestrian interaction is a conflict and the relative difference between vehicles and pedestrians speed (DeltaS) as a proxy for the crash severity **(Gettman et al., 2008)**. TTC is the minimum time-to-collision value observed during the interaction of two vehicles (or a vehicle with a pedestrian) on collision route. If at any time the TTC drops below a given threshold [2 seconds, as suggested for vehicle-pedestrian events **(Salamati et al., 2011)**] the interaction is tagged as a conflict. DeltaS is the difference in vehicle (or pedestrian) speeds observed at the instant of the minimum TTC **(Gettman et al., 2008)**.

SSAM classifies resulting conflicts into three categories based on a conflict angle (from -180° to +180°): rear end if *0°<conflict angle<30°*; crossing conflict if *85°<conflict angle<180°*; or is otherwise a lane change conflict. This angle is expressed from the perspective of the first vehicle (or pedestrian) that arrives at the conflict point and indicates the approach direction of the second vehicle **(Gettman et al., 2008)**.

To address the problem associated with pedestrian-to-pedestrian conflicts **(FHWA)**, the research team filtered out any conflict where the maximum speed was lower than 2.2 m/s (which is faster than natural walking speed).

Model Calibration and Validation

Data collected in all sites were used to calibrate and validate the simulation models. About 80% of the data were used for calibration to develop and fit the traffic model parameters, and the remaining data used for validation to assess the effectiveness of the model calibration.

Calibration of VISSIM parameters was first made by modifying driver behavior and vehicle performance parameters, and by examining their effect on traffic volumes and speeds for each link. The main driver behavior parameters of VISSIM included car-following parameters (average standstill distance, additive and multiple part of safety distance), lane-change parameters, gap acceptance parameters (minimal gap time and minimal headway), desired speed distributions and simulation resolution **(PTV AG, 2011)**.

These parameters were optimized using a genetic algorithm (Simultaneous Perturbation Stochastic Approximation – SPSA) to minimize Normalized Root Mean Square – NRMS (objective function) **(Paz, Molano, & Khan, 2014)**. The modified chi-squared statistics Geoffrey E. Havers (GEH) was used as calibration criteria. The main features of using GEH are the following: *i*) it incorporates both absolute and relative differences in comparison of estimated and observed traffic flows; *ii*) it avoids divisions by zero; and *iii*) it is independent of the order of the values **(Buisson et al., 2014)**. Fifteen simulation runs were then performed for each testing scenario, as suggested by Hale (1997). Further details about this procedure can be found in the following studies **(Paz et al., 2014)**.

Model validation focused on comparing estimated and observed flows (traffic and pedestrians), speeds, and average travel time. GEH and Mean Absolute Percent Error (MAPE) statistics were used to measure goodness of fit **(Buisson et al., 2014)**.

Scenarios

Baseline scenario is the calibrated model with the observed pedestrian and traffic demands. For all crosswalks locations, the research team modeled the centroids where pedestrians enter and leave in the coded network in the same place as the actual pedestrian location. Also, pedestrians always walked to the crosswalk.

For each site, baseline scenario was applied, assuming several possible pedestrian crosswalk locations along the mid-block section: 1) from the downstream RBT1 to the upstream of RBT2 for corridors with 2 roundabouts; and 2) from the circulatory ring of the RBT2 to the upstream of RBT3 and RBT1 on the remaining sites. In the first set of corridors (US1, SP1, PT1, PT2 and PT3), crosswalks were moved in 5-m increments [each increment allows an extra stocking capacity of 1 vehicle **(Silva et al., 2013)**]. In the second set of corridors (PT4, PT5 and PT6), nearly 25 PC1 and PC2 combinations along the mid-block section were explored by site applying 5-m increments relatively to the roundabout exit section.

After that, a relationship between pollutant emissions, delay and DeltaS, and different crosswalk locations (PC1 – corridors with 2 roundabouts; PC2 – corridors with more than 2 roundabouts) was established, as depicted in **Figure 2**. During this phase, various regression models were tested to identify whether the predictive regressions models were a good fit for the evaluated data **(Sheskin, 2011)**.

Multi-objective optimization

Objective Functions

On the basis of the scenarios presented above, the following multi-objective model was constructed to minimize pollutant emissions, vehicle delay and the relative difference between vehicles and pedestrians speed.

For a given midblock pedestrian crosswalk location and site, the first and second objectives of the model mostly reveal the vehicle driver's viewpoint, which is to minimize CO_2, CO, NO_X and HC emissions per unit distance generated by vehicles (**Equation 1**) and the average delay of each vehicle trip (**Equation 2**) along the overall network:

$$\min = \frac{\sum_{m=1}^{N_m} F_{mj}}{T_D} \quad (1)$$

Where: m = Label for second of travel (s); j = Source pollutant; F_{mj} = Emission factor for pollutant j in label for second of travel m (g/s); N_m = Number of seconds (s); T_D = Total distance travelled by vehicle (km).

$$\min = d_i^v \quad (2)$$

Where: d_i^v = control delay by vehicle (s/veh).

The third objective function is devoted to the perspective of the pedestrian safety, with the goal of minimizing relative difference between vehicles and pedestrians speed (DeltaS) which is computed from SSAM (**Equation 3**). DeltaS was obtained from crossing conflicts at the candidate pedestrian crosswalk **(Gettman et al., 2008)**.

$$\min = \text{DeltaS} \quad (3)$$

Where: DeltaS = magnitude of the difference in vehicle and pedestrians speeds (km/h).

Decision Variables

The decision variables are PC1 and PC2. They were measured from the circulatory ring delimitation of RBT2 to the limit of crosswalk (see **Figure 2** for more details).

Constraints

Equation 4 represents the available range of spacing between roundabouts (see **Table 1**) which constitutes the principal constraint for the multi-objective optimization:

$$5 \leq S \leq S_{\max} \quad (4)$$

Where: $S_{\max}$ = maximum spacing length of the analyzed site that allows a stocking capacity of 1 vehicle before the upstream of exit lane of the adjacent roundabout (m).

Solution Approach

Four multi-objective tests were optimized for each site: 1) delay-CO_2-DeltaS; 2) delay-CO-DeltaS; 3) delay-NO_X-DeltaS and 4) delay-HC-DeltaS. The regression functions were PC (PC1 or PC2 depending on the site) versus delay, PC versus CO_2 emissions, PC versus CO emissions, PC versus NO_X emissions, PC versus HC emissions, and PC versus DeltaS.

The solution of a multi-objective model is always located in its Pareto optimal (non-dominated) set. The Fast Non-Dominated Sorting Genetic Algorithm (NSGA-II) **(Deb,**

Pratap, Agarwal, & Meyarivan, 2002) was adopted in this research for six main reasons: 1) less computational complexity; 2) elitist approach; 3) emphasis on the non-dominated solutions during the process; 4) diversity preserving mechanism, 5) no requisite to consider a sharing parameter; and 6) real number encoding **(Deb et al., 2002)**. The standard flowchart of NSGA-II displayed in **Figure 3** was used.

Figure 3 Flowchart of solution algorithm based on NSGA-II.

Sensitivity analysis on the NSGA-II parameters (population size, maximum number of generations, and mutation and crossover rates) was performed before optimization to ensure the diversity in the solutions and the convergence to Pareto Optimal Front (POF) **(Konak, Coit, & Smith, 2006)**.

For the purpose of analysis, all objective variables are considered to have the same weight during the optimization procedure. NSGA-II does not take into account the different units and magnitudes of the measures involved during its procedure. This means that the set of optimal values includes values that will minimize emissions, delay and relative different between vehicles and pedestrians speed regardless of the magnitude or units of the output measure.

Results and discussion

Model Calibration and Validation

Summary statistics of the VISSIM calibrated model at the selected sites are presented in **Table 2**. The model used 15 random seed runs **(Hale, 1997)** and is based on the paired estimated-observed flows and speeds in each link. The NRMS, the GEH and MAPE goodness of fit measures, as well as average travel time for through movements are provided. Lane-change parameters were marginally unaffected by the calibration while a simulation resolution of 10 time steps per simulation seconds (second-by-second vehicle record data) was used in all sites **(PTV AG, 2011)**.

The findings showed a good fit between estimated and observed data using a linear regression analysis. Specifically, applying the site-calibrated values, R^2 values higher than 0.90 and 0.75 were produced for estimated traffic flows and speeds, respectively, against observed data. This meant that the estimated data explained more than 75% variation in the field measurements. Additionally, the calibrated critical gap times (2.9-4.2 s depending on the site) reflected countries driving habits, as presented elsewhere **(Vasconcelos, Seco, & Silva, 2013)**. The outputs of **Table 2** showed improvement of the GEH statistic with calibrated model parameters. More than 85% of the links achieved a GEH values less than 4, thereby satisfying the calibration criteria **(Dowling, Skabadonis, & Alexiadis, 2004)**, while MAPE values for the speeds ranged from 6% to 14% between PT4 and PT3 sites, respectively. The maximum average travel time difference [using 150 floating car runs **(Dowling et al., 2004)** by each through movement] was recorded at the PT3 site for South-North movement (~10%).

Table 2 Summary of calibration for the traffic model with adjusted parameters

Sites traffic operations analysis

This section quantified and compared vehicle delay, pollutant emissions (CO_2, CO, NO_X and HC) per unit distance, and DeltaS by site with the current crosswalk locations. Delay and vehicle activity data as speed, acceleration-deceleration and slope on a second-by-second basis were given from the vehicle record tool of the VISSIM model **(PTV AG, 2011)** while DeltaS was computed in SSAM **(Gettman et al., 2008)**.

Site-Specific operational, emissions and safety outputs are summarized in **Table 3**. Several conclusions about the effect of crosswalk location can be drawn. (*i*) crosswalks near the roundabout exit section (US1, PT3 and PT6) generate the highest CO_2 emissions per unit distance and the lowest DeltaS values, which agrees with the previous study conducted by **(Fernandes, Fontes, Pereira, et al., 2015)**; (*ii*) The PT3 and PT6 sites result in weak traffic performance and high emission levels among Portuguese sites, mostly because of the high pedestrian flows and the low spacing between roundabouts; (*iii*) Mid-block crosswalks from the PT1 and PT2 sites cause the highest speeds differences between vehicles and pedestrians when compared with remaining sites; (*iv*) The arterial where crosswalk is located at the SP1 site has 10% and 65% less traffic and pedestrians flows, respectively than the equivalent arterial at the PT1, but vehicles generate higher emissions per unit distance for local pollutants (more than 15%).

Table 3 Site-Specific output measures with existing crosswalk locations

Next section describes the optimization of current crosswalk locations to assess their performance. The main purpose of this step is to improve the above outputs (delay, pollutant emissions, and DeltaS). The results will then be compared with the existing crosswalk locations.

Multi-objective optimization

This section presents the main results of the multi-objective optimization of crosswalk locations. The parameters used in NSGA-II are summarized below:

- The population size (set of optimal solutions) is 10;
- The maximum number of generations is 1000;
- The crossover rate is 90%;
- The mutation rate is 10%.

These values were found appropriate to ensure the diversity in solutions and convergence to POF. **Figure 4** illustrates the POF involved through the course of the optimizations for corridors with two roundabouts by pollutant criteria. For each site, a three-dimensional scatter plot with three objective functions – emissions (x-axis), delay (y-axis), and DeltaS (z-axis) – as a function of PC1 and PC2 is exhibited. Each label in **Figure 4** is a Pareto point that represents an optimal PC1 solution of the final POF. Its value and corresponding outputs are listed in **Table 4**.

The graphs confirmed the trade-off between emissions (independent of the considered pollutant) and traffic performance, and DeltaS variables from the minimal to the maximum extremes in the set of optimal PC1. Most of solutions were located at the mid-block sub-

segments and near the circulatory ring of the roundabout (PC1<15 m). If one adopts the solution that minimizes global pollutant emissions of each site, then one could save between 1% and 6% in average CO_2 emissions at the SP1 and PT3 sites, respectively when compared with existing crosswalk locations.

The improvements in average delay at the PT3 site were particularly impressive. This site initially presented the closest crosswalk to the exit section and high pedestrian demand. For a chosen PC1 value of 96 m, 15% less delay could be reached compared with current location (PC1=7 m). As expected, crosswalks near by the roundabouts exit section yielded the lowest relative differences between vehicles and pedestrians speed. The lack of optimal PC1 values higher than 36 m at the SP1 site was possible due to right-turn bypass lane at RBT2. Accordingly, vehicles drive at low speeds along the mid-block section.

An intriguing result was detected at the PT1 and PT2 sites. In spite of having similar spacing between roundabouts, the optimal PC1 set for some pollutants was fairly different. While in the PT1 site the solutions in the approximate POFs were mostly found at the mid-block area, in the PT2 site some were located at 6 to 17 m away from the roundabout exit section. The explanations for this fact may be in the differences between sites' arterial traffic flow (PT2~235 vph/lane; PT1~590 vph/lane) together with the site's geometry. More precisely, a great portion of the vehicles is likely to be more retained by a crosswalk near the exit section under high traffic flows. Moreover, vehicles attain moderate speeds (≈35 km/h) close to the RBT1 east exit of the PT1 site (caused by small deflection angle in RBT1 east entry).

Figure 4 The approximate final Pareto front by pollutant criteria and site: a) US1; b) SP1; c) PT1; d) PT2 and e) PT3.

Table 4 Optimal crosswalk locations (PC1) of each site considering the pollutant function criteria

In corridors with more than 2 roundabouts, the final Pareto set of PC1 and PC2 dictated optimal solutions at the mid-block sub-segment and near the RBT2 exit section, as presented in **Figure 5** and **Table 5**. Optimal solutions assigned in the bottom conducted the highest emissions/delay values and lowest DeltaS; optimal solutions allocated in the upper of the graphs corresponded to the lowest emission/delay values and highest DeltaS. Between above extremes a trade-off occurred.

PT6 site generated the highest emissions reductions (2-9% depending on the pollutant) by adopting the solution 7. The findings pointed out small differences among pollutants in the optimal data set points. However, there were some aspects on the final POF that must be emphasized. In the PT4 site few solutions were found near RBT1 circulatory carriageway (high PC1 values). This happens because vehicles from the West leg to the south leg at RBT1 drive at moderate speeds, and the South RBT1 exit leg is a downhill road (slope >5%) which has a positive influence on the vehicle speed. Several solutions at the PT4 and PT5 sites were located near the circulatory ring. This can be explained by the differences of traffic and pedestrian flows between RBT1/RBT2 and RBT2/RBT3, in which in turns allows traffic to be less affected by crosswalks installed close to the RBT2 exit section.

Three general points were outlined from above findings. First, optimal crosswalk locations were mostly found at 5 to 20 m from the downstream roundabout exit section and along the mid-block segment. Second, the set of optimal crosswalk locations did not substantially vary from both the global and the local pollutants. Third, crosswalks in a same corridor (e.g. PC1 and PC2) presented different optimal locations along the respective mid-block segment.

This suggests that the spacing between roundabouts could have an important effect on the optimal crosswalk location along the mid-block section. Previous research conducted in this topic **(Fernandes, Salamati, et al., 2015)** demonstrated that, under short spacing values, drivers were not able to attain cruise speeds at mid-block section and emissions per unit distance were consistently high. However, this study did not include the influence of pedestrians in the traffic stream. This subject is then addressed in the following section.

Figure 5 The approximate final Pareto front by pollutant criteria and site: a) PT4; b) PT5; and c) PT6.

Table 5 Optimal crosswalk locations (PC1 and PC2) of each site considering the pollutant function criteria

Relationship between optimal crosswalk locations and corridor's characteristics

With above concerns in mind, the optimal crosswalk locations which minimize global and local emissions at each site were plotted against spacing. Because spacing varies among sites, data points of crosswalk locations were normalized in relation to the spacing between roundabouts by scaling between 0 and 1. Specifically, 0 is the location at the exit (circulatory ring delimitation) lane of the RBT1 (RBT2 for corridors with more than 2 roundabouts) while 1 is at the yield lane of the upstream roundabout.

The estimated regression models for each case confirmed prior predictions, as displayed in **Figure 6**. There was a good regression between relative optimized locations for CO_2, CO, NO_X and HC, and spacing between roundabouts ($R^2 > 0.72$) using exponential models. For these models, the analysis of R^2 (F-test) and the analysis of coefficients for the model (T-test) resulted in p-values lower than 0.001. This meant that the above coefficients did not take the value 0 at any significance level, and therefore the spacing and optimal crosswalk location variables were found to be significant at confidence levels higher than 99% **(Sheskin, 2011)**.

The scattered graphs show that for values lower than 100 m for the spacing, the relative location of the optimal crosswalk is approximately in 20%-30% of the spacing length. After that, the crosswalks are located near the midway position (value of 0.5), between 140 and 200 m of spacing.

It should be noted that other variables such as site-specific arterial traffic and pedestrian flow at the candidate crosswalks were fitted with spacing. Nevertheless, the regressions models resulted in weak correlations between outputs.

Figure 6 Relative location of the optimal crosswalk: (a) minimum CO_2 versus spacing; (b) minimum CO versus spacing; (c) minimum NO_X versus spacing and (d) minimum HC versus spacing.

Conclusions

This research examined the impact that different pedestrian crosswalk locations had on delay, CO_2, CO, NO_X and HC vehicular emissions, and on the relative difference between vehicles and pedestrians speed. The study covered eight roundabout corridors in three different countries, and conducted a multi-objective optimization of pedestrian crosswalks

at different locations. The research also explored the impact of the spacing between intersections on the optimal location of the crosswalks along the mid-block section. The methodology used was executed using a microsimulation traffic model paired with an emission methodology and safety model.

The findings demonstrated that the implementation of crosswalks near the circulating roadway (<10 m), which represented the current state of practice in some of the selected sites, offered advantages strictly from a pedestrian's safety point of view (low speeds). Crosswalks located near the mid-block section, however, tended to be associated with reduced delay and pollutant emissions, a finding that applied to all eight study corridors. No relevant differences in the optimal crosswalk location were noted when a specific pollutant was considered in the optimization.

In spite of modeling different vehicle fleets across the three countries, the fleet effect on the optimal crosswalk locations was minimal (optimal solutions for US1 and SP1 sites included crosswalks located 10 to 15 m from the circulatory road).

The analysis of the relative crosswalk location for different values of spacing, confirmed the impact of spacing ($R^2 > 0.72$) on optimized crosswalk locations along mid-block section. Specifically, if the spacing is lower than 100 m, optimal crosswalk location is approximately in 20%-30% of the spacing length. Otherwise, if the spacing is between 140 and 200 m, crosswalk can be located at the midway position.

Notwithstanding the small improvements on delay, emissions or safety in the majority of the sites after the optimization procedure, this study contributed to the current literature in four aspects:

- To assess the spacing between roundabouts as an influencing factor in determining the optimal crosswalk location;
- To include local pollutant criteria to account location-specific environmental concerns;
- To identify trade-offs between environmental /delay, and pedestrian safety fields;
- To supply basic design principles that help local authorities, transportation engineers, planners, and other professionals about pedestrian crosswalk location to accommodate location-specific needs and vulnerabilities.

Although this research provides measurement tools on how best to balance among competing objectives in locating the crosswalk, there are two limitations that must be highlighted. First, neither pedestrian delays nor pedestrians crossing outside the crosswalk were considered in the analysis. The second limitation is that the relationship between optimal crosswalk location and operational variables such as arterial traffic and pedestrian flow was not fully addressed.

Therefore, future work is need, namely:

- To study other corridors with different roundabout layouts (e.g. turbo-roundabouts and urban mini-roundabouts) where pedestrian activity is high;
- To conduct a sensibility analysis of the arterial traffic and pedestrian flow for each site to explore their impact on optimal crosswalk locations;
- To account and analyze the number of times that pedestrians cross outside crosswalks, especially when crosswalks are far from roundabouts (mid-block section).

- To include above geometrical, operational and driving behavior outputs in the multi-objective optimization.

ACKOWLEDGEMENTS

P. Fernandes acknowledges the support of the Portuguese Science and Technology Foundation (FCT) – Scholarship SFRH/BD/87402/2012. The authors also acknowledge to the project PTDC/EMS-TRA/0383/2014, that was funded within the project 9471-Reiforcement of RIDTI and funded by FEDER funds, and the Strategic Project UID-EMS-00481-2013.

REFERENCES

ACAP. (2014). *Automobile Industry Statistics 2013 Edition*. (ACAP – Automobile Association of Portugal).

Anya, A. R., Rouphail, N. M., Frey, H. C., & Liu, B. (2013). *Method and Case Study for Quantifying Local Emissions Impacts of Transportation Improvement Project Involving Road Realignment and Conversion to Multilane Roundabout.* Paper presented at the Transportation Research Board 92nd Annual Meeting, Washington, DC.

Brilon, W. (2016). *Safety of roundabouts: an international overview*. Paper presented at the 95th Annual Meeting of the Transportation Research Board, Washington, DC.

Bugg, Z., B., Schroeder, P., Jenior, M., Brewer, and L. Rodegerdts. (2015). *A Methodology to Compute Roundabout Corridor Travel Time*. Paper presented at the Presented at 94th Annual Meeting of the Transportation Research Board, Washington, DC.

Buisson, C., Daamen, W., Punzo, V., Wagner, P., Montanino, M., & Ciuffo, B. (2014). Calibration and validation principles. *In Traffic Simulation and Data (Eds.)* (pp. 89-118). London, UK: CRC Press.

Coelho, M. C., Frey, H. C., Rouphail, N. M., Zhai, H., & Pelkmans, L. (2009). Assessing methods for comparing emissions from gasoline and diesel light-duty vehicles based on microscale measurements. *Transportation Research Part D: Transport and Environment, 14*(2), 91-99. doi: http://dx.doi.org/10.1016/j.trd.2008.11.005

Deb, K., Pratap, A., Agarwal, S., & Meyarivan, T. (2002). A fast and elitist multiobjective genetic algorithm: NSGA-II. *Evolutionary Computation, IEEE Transactions on Evolutionary Computation, 6*(2), 182-197. doi: http://dx.doi.org/10.1109/4235.996017

DGT. Parque de Vehículos [In Spanish]. Retrieved June 18, 2015, from https://sedeapl.dgt.gob.es/IEST2/indexPortal.htm

Dhamaniya, A., & Chandra, S. (2014). Influence of Undesignated Pedestrian Crossings on Midblock Capacity of Urban Roads. *Transportation Research Record: Journal of the Transportation Research Board, 2461*, 137-144. doi: http://dx.doi.org/10.3141/2461-17

Dowling, R., Skabadonis, A., & Alexiadis, V. (2004). *Traffic analysis toolbox, volume III: Guidelines for applying traffic microsimulation software*. (FHWA-HRT-04-040, FHWA, U.S. Department of Transportation).

Duran, C., & Cheu, R. (2013). Effects of Crosswalk Location and Pedestrian Volume on Entry Capacity of Roundabouts. *International Journal of Transportation Science and Technology, 2*(1), 31-46. doi: http://dx.doi.org/10.1260/2046-0430.2.1.31

Fernandes, P., Fontes, T., Neves, M., Pereira, S. R., Bandeira, J. M., Rouphail, N. M., & Coelho, M. C. (2015). Assessment of Corridors with Different Types of

Intersections. *Transportation Research Record: Journal of the Transportation Research Board, 2503*(0), 39-50. doi: http://dx.doi.org/10.3141/2503-05

Fernandes, P., Fontes, T., Pereira, S. R., Rouphail, N. M., & Coelho, M. C. (2015). Multicriteria Assessment of Crosswalk Location in Urban Roundabout Corridors. *Transportation Research Record: Journal of the Transportation Research Board, 2517*(0), 37-47. doi: http://dx.doi.org/10.3141/2517-05

Fernandes, P., Salamati, K., Rouphail, N., & Coelho, M. C. (2015). Identification of emission hotspots in roundabouts corridors. *Transportation Research Part D: Transport and Environment, 37*(0), 48-64. doi: http://dx.doi.org/10.1016/j.trd.2015.04.026

FHWA. SSAM 2.1.6 Release Notes. Retrieved June 14, 2015, from http://www.fhwa.dot.gov/downloads/research/safety/ssam/ssam2_1_6_release_notes.cfm

Frey, H. C., Zhang, K., & Rouphail, N. M. (2010). Vehicle-Specific Emissions Modeling Based upon on-Road Measurements. *Environmental Science & Technology, 44*(9), 3594-3600. doi: http://dx.doi.org/10.1021/es902835h

Gettman, D., Pu, L., Sayed, T., & Shelby, S. G. (2008). *Surrogate safety assessment model and validation: final report.* (FHWA-HRT-08-051, FHWA, U.S. Department of Transportation).

Guo, R., & Zhang, Y. (2014). Exploration of correlation between environmental factors and mobility at signalized intersections. *Transportation Research Part D: Transport and Environment, 32*(0), 24-34. doi: http://dx.doi.org/10.1016/j.trd.2014.05.011

Hale, D. (1997). How many netsim runs are enough? *McTrans, 11*(3), 1-9.

Haley, R., Ott, S., Hummer, J., Foyle, R., Cunningham, C., & Schroeder, B. (2011). Operational Effects of Signalized Superstreets in North Carolina. *Transportation Research Record: Journal of the Transportation Research Board, 2223*, 72-79. doi: http://dx.doi.org/10.3141/2223-09

HCM. (2010). *The Highway Capacity Manual*. Transportation Research Board, Washington, DC.

Hellinga, B., & Sindi, A. (2012). Analytical Method for Estimating Delays to Vehicles Traversing Single-Lane Roundabouts as a Function of Vehicle and Pedestrian Volumes. *Transportation Research Record: Journal of the Transportation Research Board, 2312*, 56-66. doi: http://dx.doi.org/10.3141/2312-06

Isebrands, H., Hallmark, S., Fitzsimmons, E., & Stroda, J. (2008). *Toolbox to Evaluate the Impacts of Roundabouts on a Corridor or Roadway Network.* St Paul, MN: Minnesota Department of Transportation, Research Services Section, Report No. MN/RC 2008-24.

Kang, N., & Nakamura, H. (2015). Estimation of Roundabout Entry Capacity That Considers Conflict with Pedestrians. *Transportation Research Record: Journal of the Transportation Research Board, 2517*, 61-70. doi: http://dx.doi.org/10.3141/2517-07

Kang, N., Nakamura, H., & Asano, M. (2014). Estimation of Roundabout Entry Capacity Under the Impact of Pedestrians by Applying Microscopic Simulation. *Transportation Research Record: Journal of the Transportation Research Board, 2461*, 113-120. doi: http://dx.doi.org/10.3141/2461-14

Konak, A., Coit, D. W., & Smith, A. E. (2006). Multi-objective optimization using genetic algorithms: A tutorial. *Reliability Engineering & System Safety, 91*(9), 992-1007. doi: http://dx.doi.org/10.1016/j.ress.2005.11.018

Kutz, M. (2008). *Environmentally Conscious Transportation*. John Wiley & Sons, New York, US.

Kwak, J., Park, B., & Lee, J. (2012). Evaluating the impacts of urban corridor traffic signal optimization on vehicle emissions and fuel consumption. *Transportation Planning and Technology, 35*(2), 145-160. doi: http://dx.doi.org/10.1080/03081060.2011.651877

Li, S., Zhu, K., van Gelder, B., Nagle, J., & Tuttle, C. (2002). Reconsideration of Sample Size Requirements for Field Traffic Data Collection with Global Positioning System Devices. *Transportation Research Record: Journal of the Transportation Research Board, 1804*, 17-22. doi: http://dx.doi.org/10.3141/1804-03

Li, Z., DeAmico, M., Chitturi, M. V., Bill, A. R., & Noyce, D. A. (2013). *Calibration of VISSIM Roundabout Model: A Critical Gap and Follow-up Headway Approach*. Paper presented at the 92nd Annual Meeting of the Transportation Research Board, Washington, DC.

NCHRP. (2010). Roundabouts: An Informational Guide (Second Edition). National Cooperative Highway Research Program (NCHRP Report 672), Transportation Research Board, Washington, DC.

OAK Bridge Data Inventory. Transportation Energy Data Book. Retrieved June 18, 2015, from http://cta.ornl.gov/data/chapter3.shtml

Paz, A., Molano, V., & Khan, A. (2014). *Calibration of Microscopic Traffic Flow Models Considering all Parameters Simultaneously*. Paper presented at the 93th Annual Meeting of the Transportation Research Board, Washington, DC.

PTV AG. (2011). VISSIM 5.30-05 user manual. Planung Transport Verkehr AG, Karlsruhe, Germany.

Salamati, K., Rouphail, N. M., Frey, H. C., Liu, B., & Schroeder, B. J. (2015). A Simplified Method for Comparing Emissions at Roundabouts and Signalized Intersections. *Transportation Research Record: Journal of the Transportation Research Board, 3517*, 48-60. doi: http://dx.doi.org/10.3141/2517-06

Salamati, K., Schroeder, B., Rouphail, N. G., Cunningham, C., Long, R., & Barlow, J. (2011). Development and Implementation of Conflict-Based Assessment of Pedestrian Safety to Evaluate Accessibility of Complex Intersections. *Transportation Research Record: Journal of the Transportation Research Board, 2264*, 148-155. doi: http://dx.doi.org/10.3141/2264-17

Schroeder, B., Rouphail, N., Salamati, K., & Bugg, Z. (2012). Effect of Pedestrian Impedance on Vehicular Capacity at Multilane Roundabouts with Consideration of Crossing Treatments. *Transportation Research Record: Journal of the Transportation Research Board, 2312*, 14-24. doi: http://dx.doi.org/10.3141/2312-02

Sheskin, D. J. (2011). *Handbook of Parametric and Nonparametric Statistical Procedures, Fifth Ed.* Chapman & Hall/CRC, London.

Silva, A. B., Cunha, J., Relvão, T., & Silva, J. P. (2013). *Evaluation of Effect of Pedestrian Crossings on Roundabout Performance Using Microsimulation*. Paper presented at the Presented at 92nd Annual Meeting of the Transportation Research Board, Washington, DC.

Silva, A. B., Mariano, P., & Silva, J. P. (2015). Performance Assessment of Turbo-roundabouts in Corridors. *Transportation Research Procedia, 10*(0), 124-133. doi: http://dx.doi.org/10.1016/j.trpro.2015.09.062

USEPA. (2002). Methodology for developing modal emission rates for EPA's multi-scale motor vehicle & equipment emission system. Prepared by North Carolina State University for US Environmental Protection Agency, EPA420, Ann Arbor, MI.

Vasconcelos, L., Seco, A. M., & Silva, A. B. (2013). Comparison of Procedures to Estimate Critical Headways at Roundabouts. *Promet - Traffic and Transportation, 25*(1), 43-53. doi: http://dx.doi.org/10.7307/ptt.v25i1.1246

Yang, Z., Liu, P., Xu, X., & Xu, C. (2016). *Multi-objective Evaluation of Mid-block Crosswalks on Urban Streets Based on TOPSIS and Entropy Methods*. Paper presented at the 95th Annual Meeting of the Transportation Research Board, Washington, DC.

Żak, J., Meneguzzer, C., & Rossia, R. (2011). Evaluating the impact of pedestrian crossings on roundabout entry capacity. *Procedia - Social and Behavioral Sciences, 20*, 69-78. doi: http://dx.doi.org/10.1016/j.sbspro.2011.08.012

Zhai, H., Frey, H. C., & Rouphail, N. M. (2008). A Vehicle-Specific Power Approach to Speed- and Facility-Specific Emissions Estimates for Diesel Transit Buses. *Environmental Science & Technology, 42*(21), 7985-7991. doi: http://dx.doi.org/10.1021/es800208d

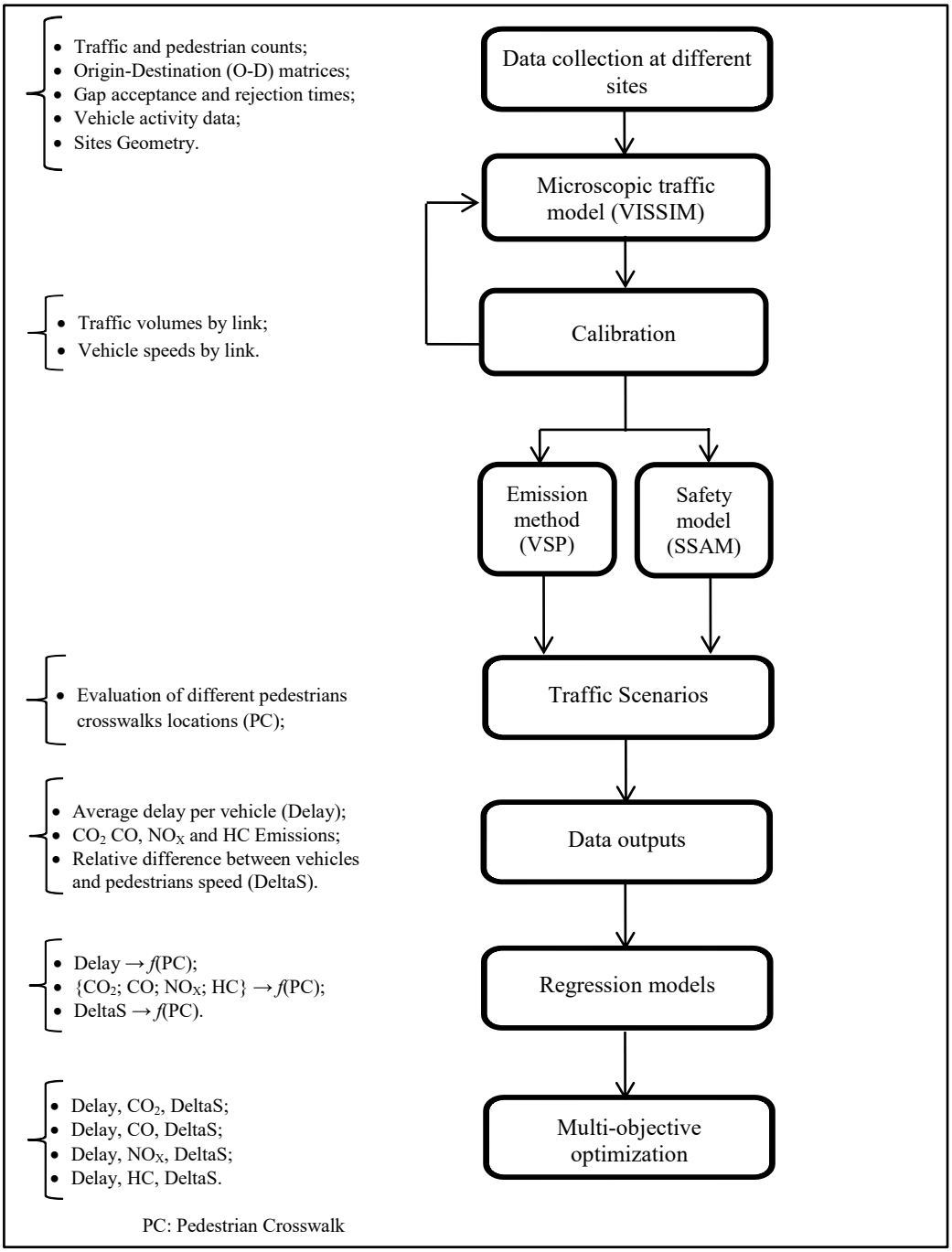

Figure 7 Methodological framework.

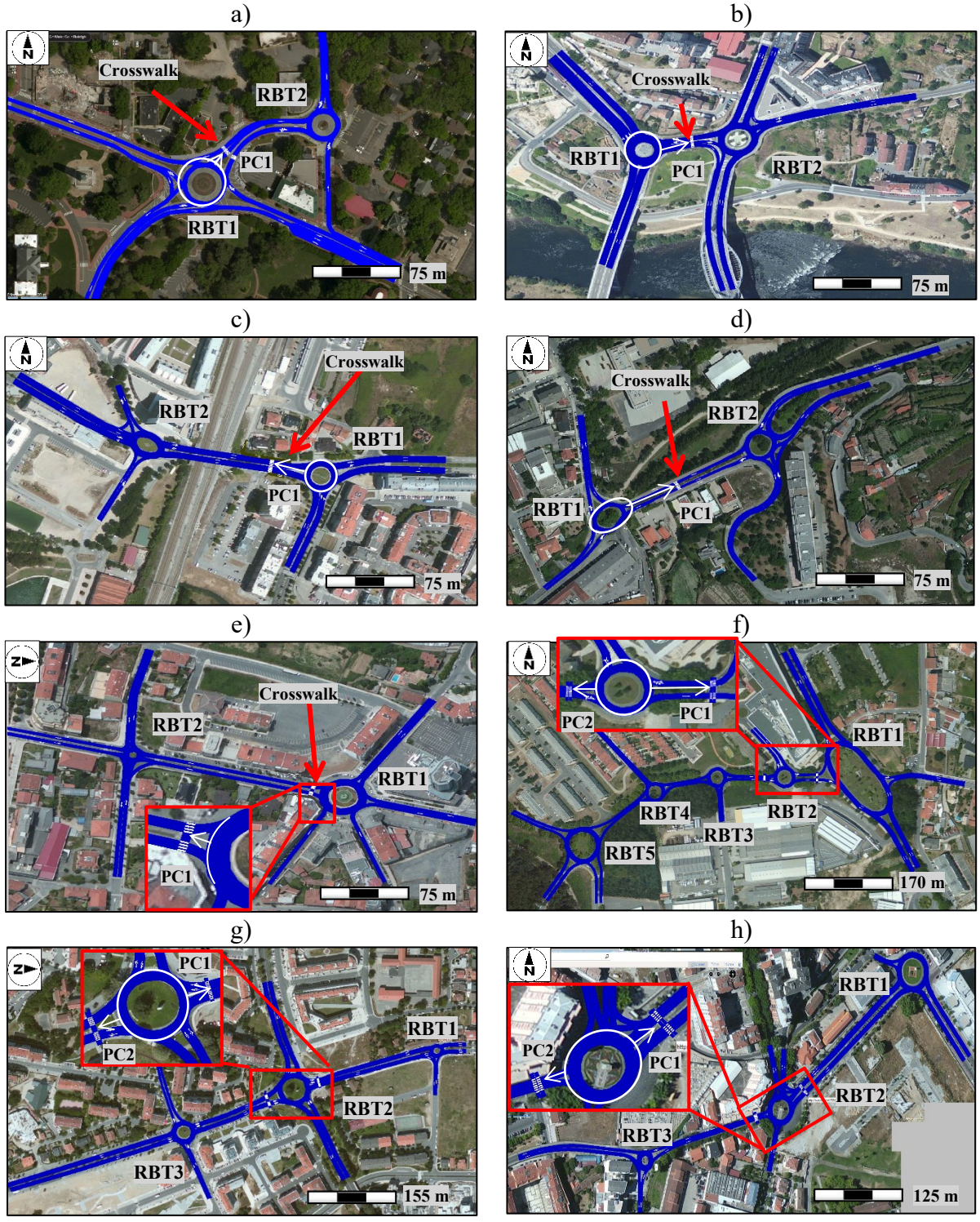

Note: *PC1 and PC2 are the distances from the RBT2 exit section to the candidate crosswalks*

Figure 8 Aerial view of the Candidate Sites: a) US1; b) SP1; c) PT1; d) PT2; e) PT3; f) PT4; g) PT5; h) PT6 [Source: https://www.bing.com/maps/].

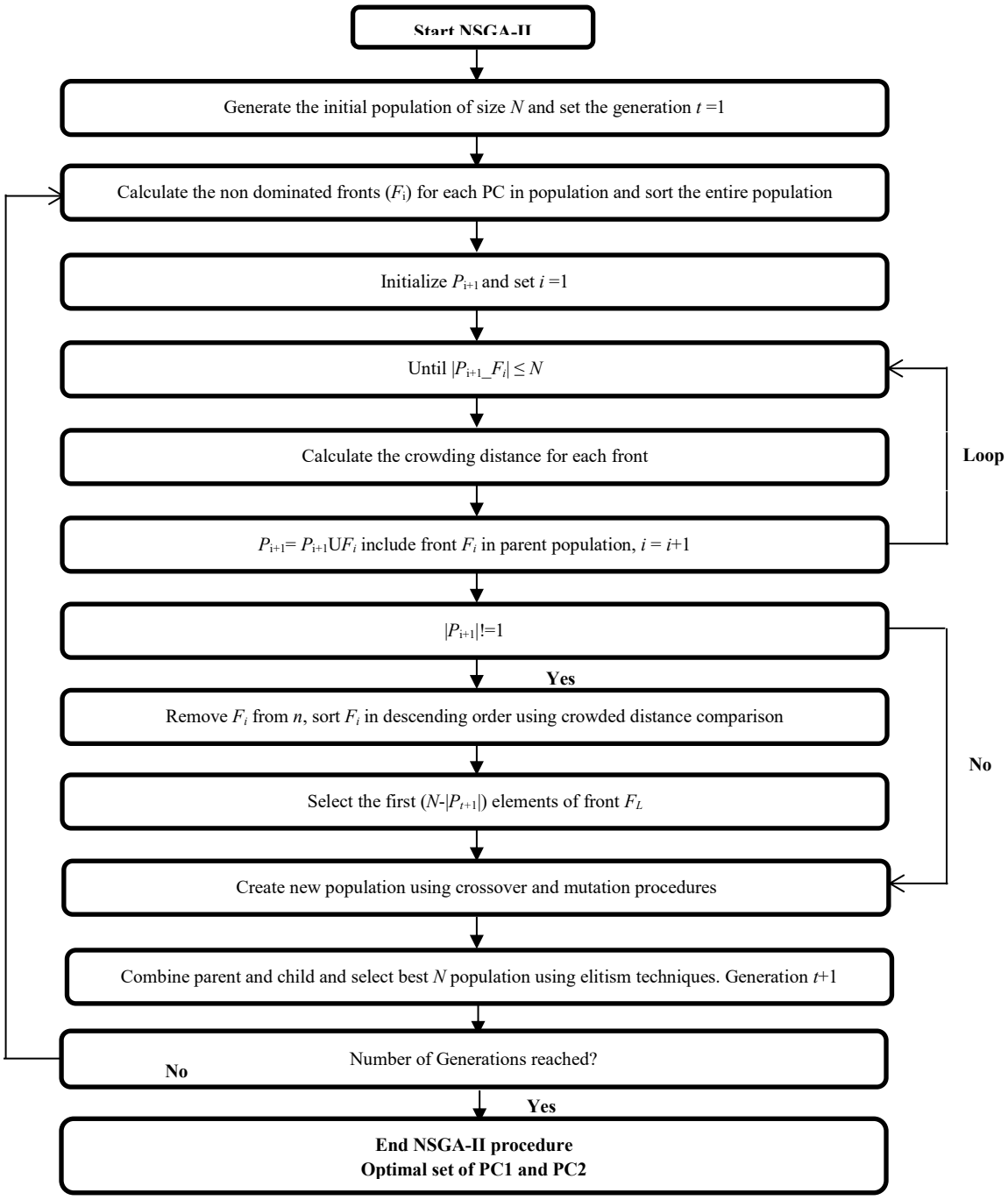

Figure 9 Flowchart of solution algorithm based on NSGA-II.

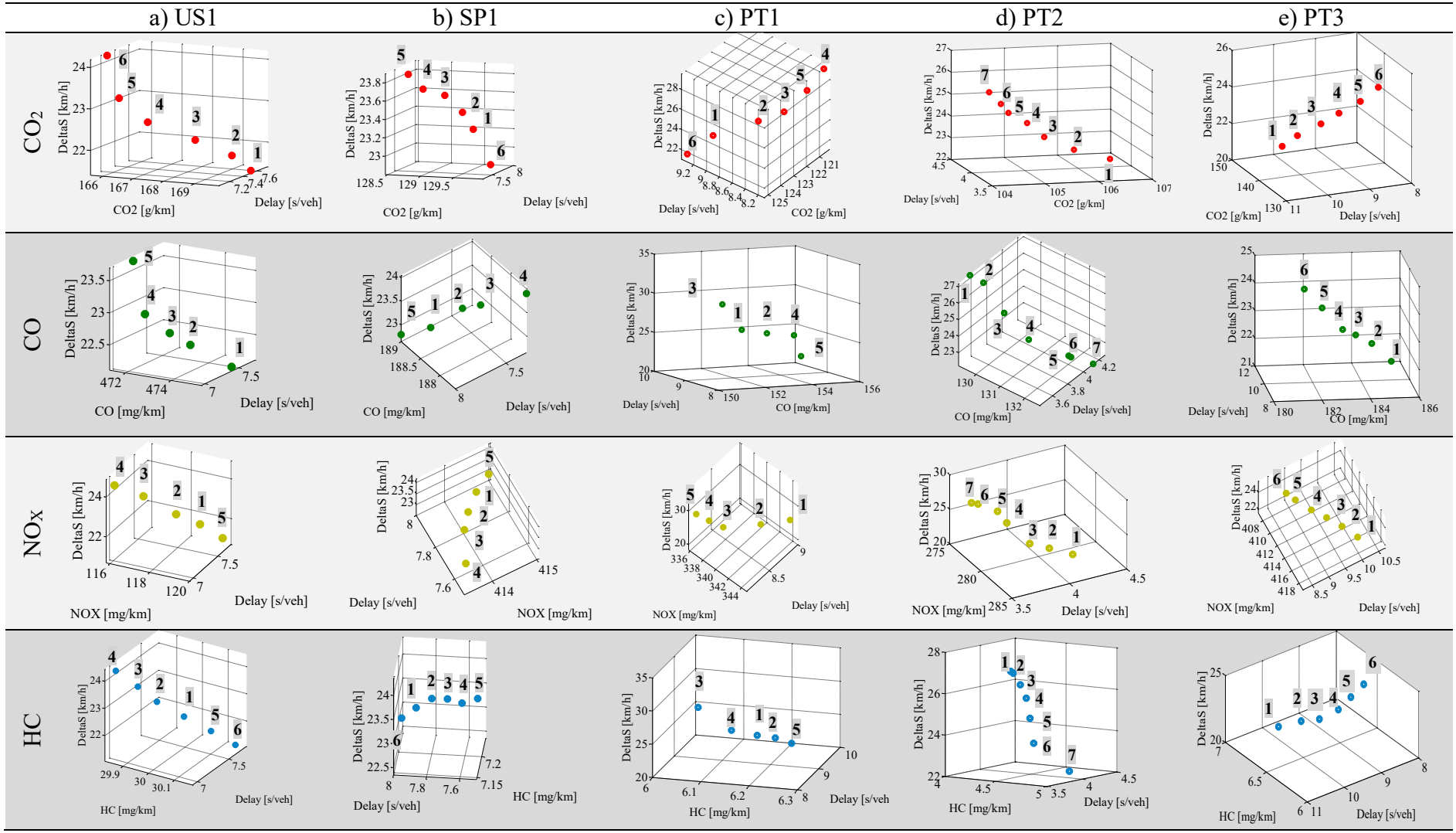

Figure 10 The approximate final Pareto front by pollutant criteria and site: a) US1; b) SP1; c) PT1; d) PT2 and e) PT3.

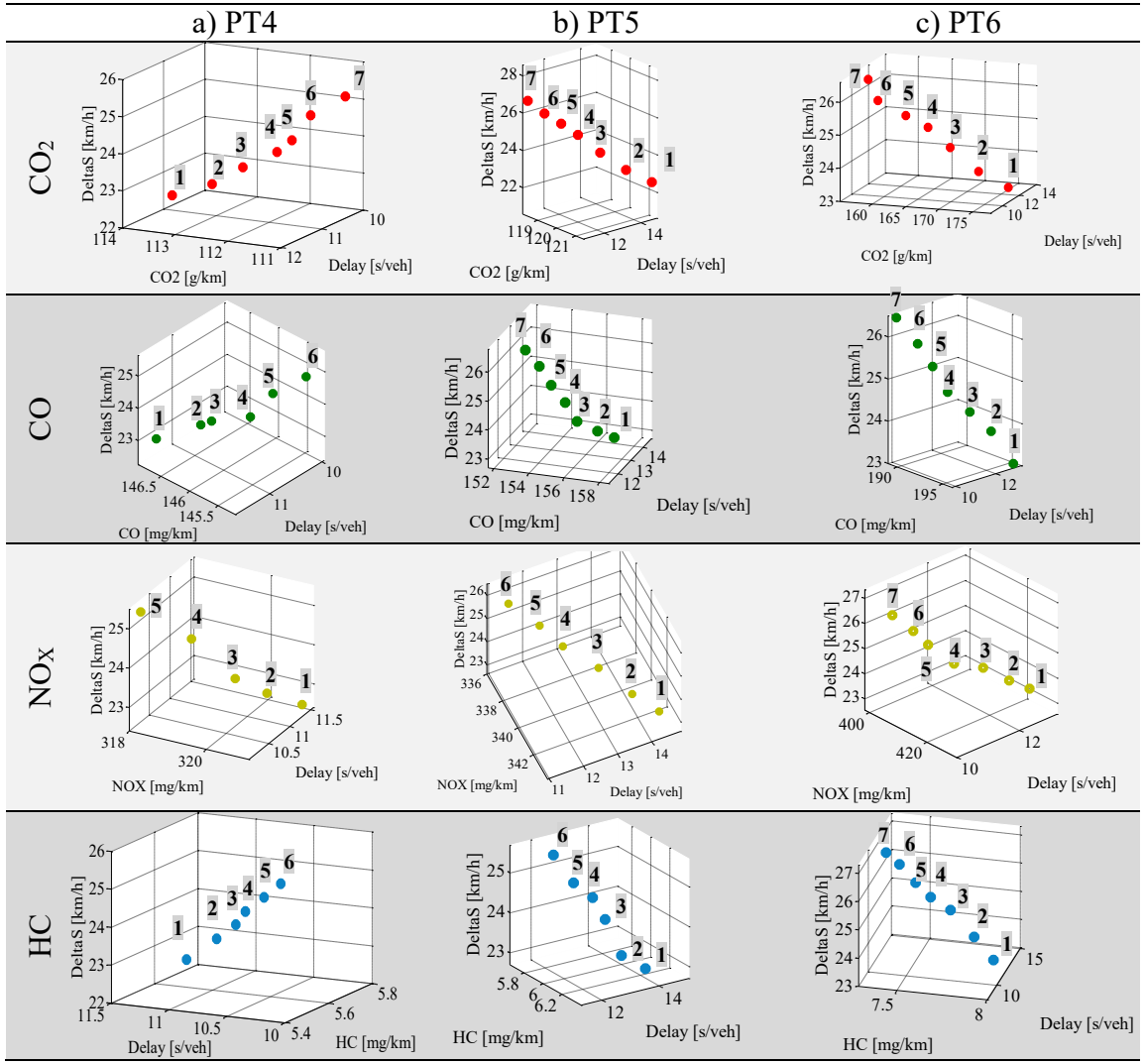

Figure 11 The approximate final Pareto front by pollutant criteria and site: a) PT4; b) PT5; and c) PT6.

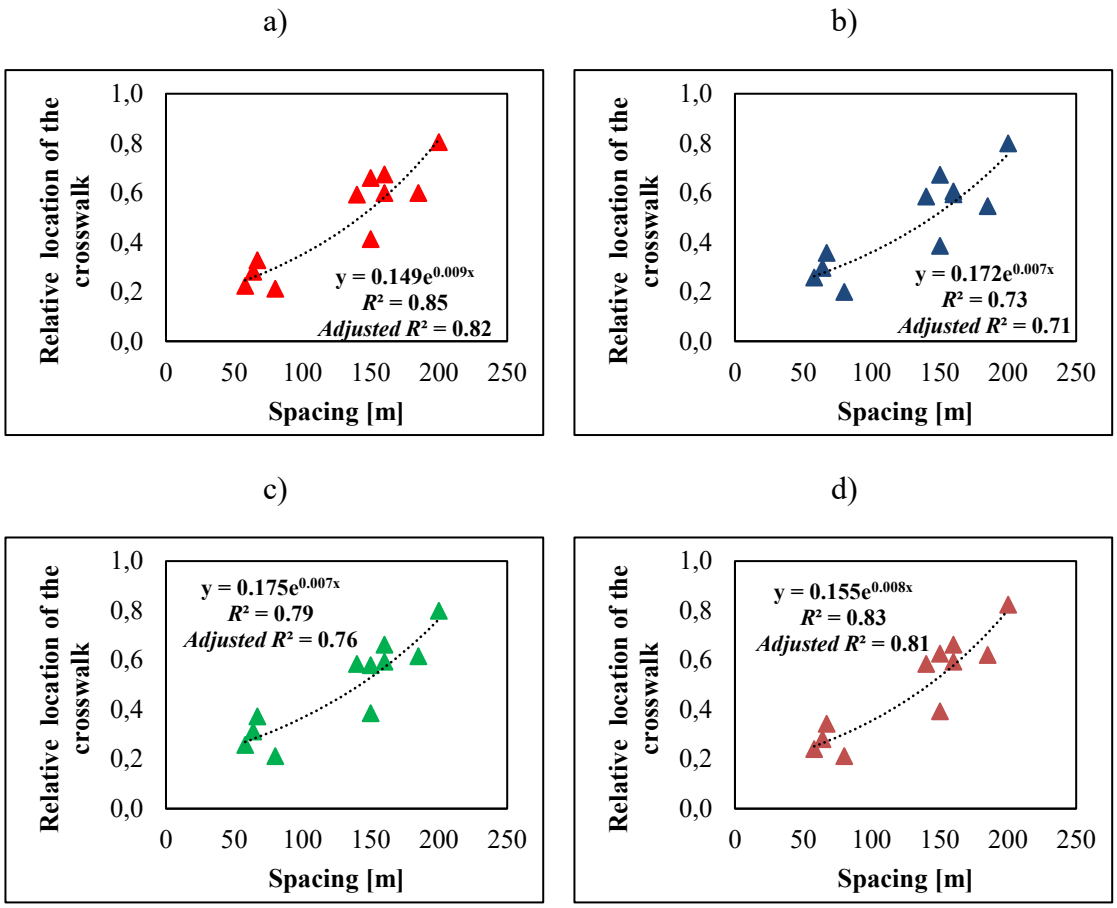

Note: *0 is the location at the exit lane of downstream roundabout and 1 is at the yield lane of upstream roundabout considering the mid-block section where crosswalk is located.*

Figure 12 Relative location of the optimal crosswalk: (a) minimum CO_2 versus spacing; (b) minimum CO versus spacing; (c) minimum NO_X versus spacing; and (d) minimum HC versus spacing.

Table 6 Summary of Study Sites

City	Site ID	Rbts. ID	Arterial number of lanes	Number of circulating lanes	Number of entry/exit legs	Circle Inscribed Diameter [m]	Spacing [m]	Crosswalks Location [m]	Crosswalk Treatment solution	Crosswalk GPS Coordinates	Peak pedestrian flow [p/h]	Peak arterial flow [vph/lane][a]
Raleigh, NC	US1	RBT1	1	1	4/4	36	80	7	Raised	35°47'10.75"N 78°39'43.87"W	110	480
		RBT2	1	1	3/2	30						
Orense	SP1	RBT1	3	2	3/3	38	58	30	Not Raised	42°20'49.5"N 7°52'28.6"W	85	315
		RBT2	2	2	4/4	45						
Aveiro	PT1	RBT1	2	2	3/3	41	150	33	Raised	40°38'26.7"N 8°38'27.4"W	110	590
		RBT2	2	2	4/4	41 and 32[b]						
Guimarães	PT2	RBT1	1	1	3/3	41 and 26[c]	140	55	Raised	41°26'39.6"N 8°16'59.4"W	120	235
		RBT2	1	1	4/4	36						
Oliveira de Azeméis	PT3	RBT1	1	2	4/4	48	160	7	Raised	40°50'16.9"N 8°28'47.0"W	195	630
		RBT2	1	1	4/4	29						
São João da Madeira	PT4[d]	RBT1	1/2	2	4/4	126 and 61[b]	64	27	Raised	40°53'13.1"N 8°29'27.6"W	120	465
		RBT2	1	1	3/3	39	67	12[e]	Raised	40°53'13.07"N 8°29'31.03"W	75	345
		RBT3	1	1	3/3	36	72	-		-	-	445
		RBT4	1	1	3/3	36	100	-		-	-	340
		RBT5	1	1	4/4	56	-	-		-	-	-
Viseu	PT5	RBT1	2	2	3/3	24	200	13	Raised	40°38'58.68"N 7°54'44.23"W	65	275
		RBT2	2	2	4/4	56	160	17[e]	Raised	40°38'55.9"N 7°54'43.0"W	135	585
		RBT3	2	2	4/4	40	-	-		-	-	-
Chaves	PT6	RBT1	1	2	3/3	45	185	15	Raised	41°44'39.80"N 7°28'14.06"W	165	265
		RBT2	1/2	2	5/5	34	105	10[e]	Not Raised	41°44'38.8"N 7°28'16.5"W	180	515
		RBT3	2	2	3/3	23	-	-		-	-	-

[a] *Arterial traffic at the mid-block areas between roundabouts;*

[b] *Oval roundabouts; therefore, there are two values for the inscribed diameter;*

[c] *Roundabout RBT1 has two semi-circles;*

[d] *There are only two crosswalks between downstream of RBT1 and the upstream of RBT5;*

[e] *Distance from the RBT2 exit section.*

Table 7 Summary of calibration for the traffic model with adjusted parameters

Site ID	Parameter	Value	NRMS	GEH	R^{2a}	MAPE	Travel time [sec][b]
US1	Average standstill distance Additive part of safety Multiple part of safety Minimal gap time (s)	0.9 1.0 1.1 4.3	0.549	< 4 for 93 % of the links	Flows: 0.95 Speeds: 0.85	Flows: 3.3% Speeds:11.1%	Observed NS: 51.1±10.6 Estimated NS: 54.0±3.3 Observed SN: 41.6±7.0 Estimated SN: 44.4±2.5
SP1	Average standstill distance Additive part of safety Multiple part of safety Minimal gap time (s)	1.0 1.2 1.4 3.4	0.307	< 4 for 96 % of the links	Flows: 0.94 Speeds: 0.81	Flows: 2.9% Speeds:10.2%	Observed WE: 50.5±5.2 Estimated WE: 52.6±2.0 Observed EW: 55.1±9.3 Estimated EW: 50.9±1.5
PT1	Average standstill distance Additive part of safety Multiple part of safety Minimal gap time (s)	1.1 0.9 1.8 2.9	0.479	< 4 for 91% of the links	Flows: 0.92 Speeds: 0.76	Flows: 6.0% Speeds:12.8%	Observed WE: 51.9±3.6 Estimated WE: 51.2±1.6 Observed EW: 47.1±5.0 Estimated EW: 48.6±2.6
PT2	Average standstill distance Additive part of safety Multiple part of safety Minimal gap time (s)	1.1 1.3 1.8 3.1	0.174	< 4 for 96 % of the links	Flows: 0.91 Speeds: 0.88	Flows: 7.0% Speeds:9.4%	Observed WE: 50.1±3.8 Estimated WE: 52.3±1.5 Observed EW: 52.0±1.7 Estimated EW: 49.0±2.2
PT3	Average standstill distance Additive part of safety Multiple part of safety Minimal gap time (s)	1.0 1.0 1.2 3.1	0.355	< 4 for 95 % of the links	Flows: 0.93 Speeds: 0.80	Flows: 3.4% Speeds:13.7%	Observed NS: 61.9±6.0 Estimated NS: 58.1±3.4 Observed SN: 59.9±5.6 Estimated SN: 53.6±2.0
PT4	Average standstill distance Additive part of safety Multiple part of safety Minimal gap time (s)	1.0 0.9 1.3 3.3	0.247	< 4 for 92 % of the links	Flows: 0.92 Speeds: 0.86	Flows: 5.0% Speeds:6.4%	Observed WE: 87.5±6.7 Estimated WE: 89.9±1.3 Observed EW: 83.9±7.5 Estimated EW: 89.1±1.9
PT5	Average standstill distance Additive part of safety Multiple part of safety Minimal gap time (s)	1.1 1.0 1.3 3.2	0.232	< 4 for 92 % of the links	Flows: 0.93 Speeds: 0.85	Flows: 2.8% Speeds:8.6%	Observed NS: 90.2±3.0 Estimated NS: 92.3±2.2 Observed SN: 89.9±5.2 Estimated SN: 87.7±1.0
PT6	Average standstill distance Additive part of safety Multiple part of safety Minimal gap time (s)	1.0 1.2 2.2 3.2	0.410	< 4 for 100 % of the links	Flows: 0.95 Speeds: 0.88	Flows: 4.6% Speeds:10.4%	Observed WE: 82.6±9.3 Estimated WE: 85.6±2.1 Observed EW: 91.3±6.5 Estimated EW: 86.9±1.7

a Linear regression analysis between the estimated and the observed flows and speeds on each coded link;

b The relative difference between estimated and observed travel time was computed using the following equation: 100× (Estimated Travel Time – Observed Travel Time) / Observed Travel Time.

Notes: *WE – West to East movement: EW – East to West movement: NS – North to South movement; SN – South to North movement*

Table 8 Site-Specific output measures with existing crosswalk locations

Site ID	Capacity	Emissions				Safety
	Delay [s/veh]	CO_2 [g/km]	CO [mg/km]	NO_X [mg/km]	HC [mg/km]	DeltaS [km/h]
US1	7.8	170	478	121	32.79	22.0
SP1	7.9	129	189	414	7.21	23.0
PT1	8.3	122	153	340	6.19	27.0
PT2	3.8	105	130	277	4.61	26.1
PT3	10.1	140	185	415	6.61	21.4
PT4	10.7	114	146	320	5.74	22.8
PT5	12.5	120	155	340	6.11	24.0
PT6	11.2	174	194	419	7.82	22.8

Table 9 Optimal crosswalk locations (PC1) of each site considering the pollutant function criteria

Site ID	Solution [a]	PC1 [m]	CO_2 [g/km]	Delay [s/veh]	DeltaS [km/h]	PC1 [m]	CO [mg/km]	Delay [s/veh]	DeltaS [km/h]	PC1 [m]	NO_X [mg/km]	Delay [s/veh]	DeltaS [km/h]	PC1 [m]	HC [mg/km]	Delay [s/veh]	DeltaS [km/h]
US1	1	**8**	168.0	7.5	22.1	**8**	475.0	7.5	22.1	**8**	119.1	7.5	22.1	**9**	30.02	7.4	22.4
	2	**10**	166.9	7.3	22.6	**9**	473.5	7.4	22.4	**11**	118.4	7.3	22.9	**11**	29.94	7.3	22.9
	3	**12**	166.2	7.2	23.2	**10**	472.9	7.3	22.6	**13**	117.0	7.2	23.7	**13**	29.89	7.2	23.5
	4	**17**	165.8	7.1	24.2	**11**	472.1	7.2	22.9	**17**	115.8	7.1	24.2	**17**	29.83	7.1	24.1
	5	**70**	169.2	7.5	21.8	**16**	471.6	7.2	23.7	**72**	120.0	7.6	21.4	**70**	30.10	7.5	21.9
	6	**72**	169.6	7.6	21.4	N/A				N/A				**72**	30.17	7.6	21.4
SP1	1	**7**	129.4	7.9	23.2	**7**	188.5	7.9	23.2	**7**	414.5	7.9	23.2	**7**	7.21	7.9	23.2
	2	**8**	129.3	7.8	23.4	**9**	188.2	7.7	23.6	**8**	414.1	7.8	23.4	**8**	7.20	7.8	23.5
	3	**9**	129.1	7.7	23.6	**10**	188.0	7.6	23.7	**9**	413.8	7.7	23.6	**9**	7.19	7.7	23.6
	4	**10**	128.9	7.5	23.7	**15**	187.6	7.3	23.9	**15**	413.4	7.5	23.9	**10**	7.17	7.6	23.7
	5	**13**	128.8	7.3	23.9	**36**	189.0	8.0	22.8	**36**	415.0	8.0	22.8	**14**	7.16	7.5	23.9
	6	**36**	129.6	8.0	22.8	N/A				N/A				**36**	7.23	8.0	22.8
PT1	1	**7**	124.8	9.0	24.1	**35**	151.4	8.3	27.1	**7**	343.6	9.0	24.1	**7**	6.21	9.0	24.1
	2	**19**	123.3	8.6	25.3	**55**	152.6	8.4	26.3	**13**	341.7	8.7	24.9	**35**	6.15	8.3	27.1
	3	**35**	121.0	8.3	27.1	**58**	150.3	8.1	30.8	**35**	339.4	8.3	27.1	**58**	6.09	8.1	30.8
	4	**62**	120.2	8.2	28.8	**92**	153.9	8.5	25.7	**58**	338.1	8.2	28.8	**98**	6.19	8.6	25.6
	5	**99**	122.3	8.4	25.9	**115**	155.3	9.3	21.8	**62**	337.0	8.1	30.8	**105**	6.23	9.3	22.4
	6	**115**	125.3	9.3	21.8	N/A				N/A				N/A			
PT2	1	**6**	106.7	4.13	22.2	**6**	132.6	4.13	22.2	**6**	283.1	4.13	22.2	**6**	4.79	4.13	22.2
	2	**9**	105.9	3.97	22.9	**9**	132.2	3.97	22.9	**9**	282.1	3.98	22.9	**17**	4.65	3.82	23.7
	3	**11**	105.3	3.92	23.6	**10**	132.2	3.94	23.1	**13**	281.2	3.86	23.4	**40**	4.63	3.80	24.9
	4	**17**	104.9	3.82	24.4	**22**	131.1	3.77	23.9	**36**	278.6	3.80	24.6	**52**	4.62	3.76	25.9
	5	**53**	104.5	3.75	25.0	**36**	130.0	3.80	24.6	**52**	277.9	3.76	25.9	**63**	4.61	3.69	26.6
	6	**63**	104.3	3.68	25.5	**58**	129.4	3.72	26.3	**75**	277.3	3.62	27.1	**82**	4.60	3.60	27.2
	7	**83**	104.0	3.58	26.2	**83**	129.3	3.58	27.2	**83**	277.0	3.58	27.2	**83**	4.59	3.58	27.3
PT3	1	**5**	142.2	10.4	21.4	**6**	185.3	10.2	21.6	**6**	416.0	10.2	21.7	**6**	6.71	10.2	21.6
	2	**7**	140.2	10.1	22.0	**9**	184.4	9.8	22.4	**9**	414.4	9.8	22.4	**9**	6.57	9.9	22.3
	3	**12**	138.7	9.6	22.8	**12**	183.7	9.6	22.8	**12**	412.9	9.6	22.8	**11**	6.44	9.7	22.8
	4	**18**	137.2	9.2	23.5	**15**	183.1	9.3	23.1	**16**	411.4	9.3	23.2	**17**	6.39	9.3	23.3
	5	**34**	135.0	8.9	24.2	**29**	182.2	9.0	24.0	**30**	410.0	9.0	24.0	**30**	6.37	9.0	24.0
	6	**96**	132.6	8.6	24.8	**95**	181.4	8.7	24.8	**96**	408.9	8.7	24.8	**94**	6.35	8.7	24.7

a Number of non-dominated solutions

Shadow cells indicate the minimal objective value for a specific crosswalk location

N/A: Not Applicable

Table 10 Optimal crosswalk locations (PC1 and PC2) of each site considering the pollutant function criteria

Site ID	Solution[a]	PC1/ PC2 [m]	CO_2 [g/km]	Delay [s/veh]	DeltaS [km/h]	PC1/ PC2 [m]	CO [mg/km]	Delay [s/veh]	DeltaS [km/h]	PC1/ PC2 [m]	NO_X [mg/km]	Delay [s/veh]	DeltaS [km/h]	PC1/ PC2 [m]	HC [mg/km]	Delay [s/veh]	DeltaS [km/h]
PT4	1	**40/5**	113.6	11.3	22.6	**40/5**	146.9	11.3	22.6	**40/29**	321.1	11.3	22.6	**40/29**	5.64	11.3	22.6
	2	**40/6**	113.0	11.1	22.9	**40/26**	146.6	11.1	23.0	**35/12**	320.4	11.1	23.0	**5/22**	5.62	11.0	23.3
	3	**5/20**	112.5	11.0	23.4	**5/24**	146.3	10.9	23.4	**5/21**	319.8	10.9	23.4	**35/18**	5.60	10.8	23.8
	4	**35/18**	112.0	10.8	23.8	**35/51**	145.9	10.6	23.8	**35/35**	319.1	10.5	24.6	**35/21**	5.59	10.7	24.2
	5	**35/24**	111.8	10.7	24.1	**35/36**	145.6	10.5	24.5	**18/22**	318.0	10.3	25.2	**35/38**	5.57	10.5	24.7
	6	**35/40**	111.6	10.5	24.7	**19/24**	145.2	10.3	25.2			N/A		**18/23**	5.54	10.3	25.2
	7	**18/22**	111.1	10.3	25.2			N/A								N/A	
PT5	1	**5/5**	121.4	14.6	22.6	**5/6**	156.6	14.4	22.7	**5/5**	342.1	14.6	22.6	**5/6**	6.13	14.4	22.7
	2	**5/17**	120.9	13.7	23.3	**125/5**	156.0	13.9	23.1	**5/15**	341.3	14.0	23.2	**125/6**	6.09	13.7	23.1
	3	**125/11**	120.3	12.9	24.2	**125/8**	155.2	13.4	23.6	**45/130**	340.5	13.2	24.3	**45/51**	6.04	13.3	24.0
	4	**85/138**	119.6	12.4	25.0	**85/115**	154.8	13.0	24.4	**85/133**	339.4	12.4	25.0	**45/76**	6.03	12.9	24.6
	5	**200/132**	119.1	12.0	25.5	**85/132**	154.5	12.3	25.3	**200/106**	338.6	11.9	25.7	**85/133**	5.98	12.4	25.0
	6	**85/108**	118.7	11.5	26.0	**125/38**	154.1	11.9	26.1	**165/106**	337.7	11.2	26.5	**160/106**	5.92	11.9	25.7
	7	**161/108**	118.2	11.1	26.6	**165/97**	153.6	11.5	26.8			N/A				N/A	
	8		N/A				N/A										
PT6	1	**5/5**	174.5	13.2	23.0	**5/5**	195.3	13.2	23.0	**5/5**	420.8	13.2	23.0	**5/5**	7.90	13.2	23.0
	2	**5/21**	170.7	12.7	23.5	**5/15**	194.4	12.5	23.8	**5/15**	419.1	12.7	23.5	**5/36**	7.81	12.6	23.9
	3	**40/6**	167.5	11.9	24.3	**5/28**	193.6	11.8	24.3	**5/26**	417.7	12.0	24.3	**110/138**	7.69	12.1	24.9
	4	**140/103**	165.2	11.1	25.0	**40/115**	192.7	11.1	24.8	**40/113**	415.3	11.3	24.7	**140/9**	7.60	11.3	25.5
	5	**140/36**	162.5	10.6	25.4	**140/15**	191.9	10.7	25.4	**140/7**	411.7	10.8	25.5	**40/38**	7.53	10.8	26.1
	6	**75/83**	159.1	10.0	25.9	**110/12**	190.9	10.4	25.9	**110/129**	409.8	10.5	26.1	**75/107**	7.45	10.4	26.8
	7	**111/99**	158.3	9.5	26.6	**100/101**	189.7	9.9	26.5	**114/87**	408.0	10.0	26.9	**115/94**	7.39	9.9	27.3

a Number of non-dominated solutions

Shadow cells indicate the minimal objective value for a specific crosswalk location

N/A: Not Applicable